# MULTIMODAL MRI-BASED TISSUE CLASSIFICATION IN BREAST DUCTAL CARCINOMA

C. Andrés Méndez*, Francesca Pizzorni Ferrarese*, Paul Summers†
Giuseppe Petralia†, Massimo Bellomi†, Gloria Menegaz*

* Department of Computer Science, University of Verona, Italy
† Department of Radiology, European Institute of Oncology, Milan, Italy

## ABSTRACT

In this paper we propose a pipeline to integrate breast diffusion and perfusion MRI for diagnosis, surgical planning and follow-up. Dynamic contrast enhanced (DCE) and diffusion weighted (DWI) MRI provide complementary information on the tissue structure and properties: while DCE-MRI allows the characterization of the lesion angiogenesis, DWI techniques can probe the apparent diffusion coefficient (ADC) and therefore assess the nature and cellularity of the lesions. Here we propose a two-step process for the integration of these modalities. First, dissimilarity-based clustering is performed on DCE-MRI to identify the different tumoral subregions. These are then mapped onto the DWI images following inter-modal registration. The probability density functions (PDFs) of the so-identified subregions in the ADC map are extracted and compared through non-parametric testing. Results show that subregions corresponding to different clusters hold statistically different PDFs,indicating a degree of consistency in the information obtained from the two modalities while providing a posterior validation of the registration method. This enables the efficient integration of the information brought by DCE and DWI, respectively, while taking advantage of their complementarity.

***Index Terms*—** multimodal registration, dissimilarity-based clustering, diffusion MRI, dynamic contrast enhanced MRI

## 1. INTRODUCTION

The best therapeutic plan for breast cancer depends on the appropriate evaluation of multiple factors for each patient. Mammography (MMG) and whole-breast ultrasonography (US) remain the conventional imaging modalities to determine the extent of tumor involvement in breast tissue. MMG screening has led to the detection of earlier breast cancers allowing women to undergo a breast-conseing surgery with no reduction in survival [1]. The challenge now is to reduce the number of multiple re-excisions and also to avoid recurrence caused by residual disease. Recent works [2] have shown that preoperative MRI evaluation of breast cancer at local extent significantly alters the rate of mastectomy and axillary lymph node resection.

In the current study, we propose the multi-modal integration of the information provided by DCE-MRI and DWI of the breast cancer lesions. First, dissimilarity-based clustering is performed on selected DCE-MRI images to identify the different types of enhancement patterns inside the tumor. Then, the resulting regions are mapped onto the corresponding ADC images, which are spatially registered through the use of a multi-resolution ellastic registration protocol. Statistical analysis revealed that the PDFs of the subregions corresponding to different clusters are statistically independent, which indicates the self-consistency of the approach and enables the integration of the information gathered from the two modalities for a robust tissue classification.

This paper is organized as follows. Section 2 describes the pipeline including the clustering and registration processing steps. Section 3 presents and discusses the results and Section 4 derives conclusions.

## 2. MATERIALS AND METHODS

This Section provides an overview on the pipeline shown in Fig. 1 and details the methodological choices with respect to both clustering and registration.

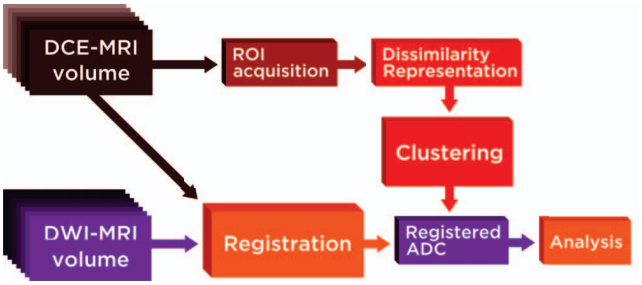



**Fig. 1**. Perfusion/Diffusion analysis and integration pipeline

The DCE-MRI data are first visually inspected to identify the images where the lesion can be detected. Clustering is performed based on perfusion curves in order to both detect the region of interest (ROI) and separate the different enhance-

ment patterns inside it. Multi-modal registration is performed between DWI and DCE-MRI data, allowing a spatial mapping of the ROI and its subregions to the DWI. Statistical analysis is performed on the ADC to test the consistency of the information provided by this modality with that extracted from the DCE-MRI, which can thus be profitably integrated for an accurate tissue characterization.

### 2.1. Data

Data were acquired from 17 patients (age $50\pm13.2$). All the patients were affected by primary ductal carcinoma, 15 having infiltrating and 2 lobular tumors.

DWI was acquired with a single-shot spin-echo (SE) echo planar imaging (EPI) sequence in three orthogonal diffusion encoding directions ($x$, $y$ and $z$) using 4 $b$ values (0, 250, 500 and 1000 $s/mm^2$) with parallel imaging (acceleration factor 2). Subjects were breathing freely, with no gating applied. The dataset consisted of 30 transverse slices (slice thickness $5\,mm$, no slice gap) and TR/TE $4800/71\,ms$, matrix $90\times150$ over the field of view (FOV) $184.5 \times 307.5\,mm$.

DCE-MRI was performed using a T1-weighted 3D FLASH sequence (TR/TE $7.4/4.7\,ms$) with a flip angle of 25 $^\circ$ and an acquisition matrix of $384 \times 384 \times 128$ and field of view (FOV) $340\times340\times166\,mm$. Each 120-slice set was collected in 90 $s$ at 8 time points for approximately 12 min of scanning. A catheter placed within an antecubital vein delivered $0.1$ $mmol/kg$ of the contrast agent, gadopentetate dimeglumine, (Magnevist, Wayne, NJ, USA) over 20 $s$ (followed by saline flush) after the acquisition of one baseline dynamic scan.

### 2.2. Dissimilarity based clustering

Dissimilarity based clustering was applied to the perfusion curves in a voxel-wise manner. From amongst the abundance of features that have been proposed as the basis for classifying lesions from breast DCE-MRI, the raw time series were used in this study. For the sake of completeness the most relevant contributions in this respect are summarized hereafter. Lavini *et al.* [6] proposed a general set of kinetic features for DCE-MRI data where time-intensity curves are classified voxel by voxel according to their shape. Kuhl *et al.* [5] showed that the use of curve shape descriptors based on the three-time-points (3TP) method could distinguish malignant from benign lesions. This method, first proposed in [3], is based on using high-spatial-resolution images while scanning the images at the selected three time points (one pre-contrast and two post-contrast time points). However, the 3TP method was criticized for not considering enhancement patterns at full time points. Subsequent pattern recognition proposals for DCE-MRI data have mainly relied on the extraction of kinetic features from the time-intensity curves or their combination with morphometric features. Gal *et al.* [4] made a survey of the available methods in the literature and proposed a set of features which includes morphological, textural and kinetic descriptors, together with variations of existing ones.

In all the methods that can be found in literature, the representation of time-intensity curves is performed by features defining a vectorial space. In this work a different approach is followed exploiting dissimilarity based representations (DBR) [8]. The concept of dissimilarity based representations consist in focusing on the contrast, or distance, between objects and in measuring it by a suitable criterion. Objects in this space are characterized thorough pairwise dissimilarities. In other words, instead of an absolute characterization of objects by a set of features, problem-centric knowledge is used to define a measure that estimates the dissimilarity between objects. A key concept in DBR is that of a *proximity relation* between two objects, which may not be explicitly represented in a feature space.

In this framework, the first step is to construct a dissimilarity matrix. This consists of a set of row vectors, one for each object. These vectors represent the objects in a vector space constructed by the dissimilarities to each other object. Usually, this vector space can be safely treated as an Euclidean space equipped with the standard inner product definition.

Let $X = \{x_1, \ldots, x_n\}$ be a set of voxel based perfusion curves. Given a dissimilarity function, a data-dependent mapping $D$ is defined as $D(\cdot, R) : X \rightarrow \mathbb{D}^n$ linking $X$ to the so-called dissimilarity space [7]. The complete dissimilarity representation yields a square matrix consisting of the dissimilarities between all pairs of objects, such that every object is described by an $n$-dimensional dissimilarity vector $D(x, X) = [d(x, x_1) \ldots d(x, x_n)]^T$ .

A distance function $D_k$ based on the adaptive dissimilarity index first proposed in [12] was used to calculate the pairwise proximity between perfusion curves. This measure covers the proximity with respect to values as well as the temporal correlation for the proximity versus behavior, and is defined as

$$D_k(S_1, S_2) = \frac{2}{1 + exp(k\textsc{Cort}(S_1, S_2))} dH(S_1, S_2) \quad (1)$$

where $S_1 = (u_1, \ldots, u_p)$ and $S_2 = (v_1, \ldots, v_p)$ are two voxel-derived perfusion curves obtained at acquisition times $(t_1, \ldots, t_p)$, and $k$ is a modulating parameter [12, 11]. CORT is the temporal correlation, $dH$ is the Hausdorff distance between curves (eq. 3), defined respectively as follows

$$\textsc{Cort}(S_1, S_2) = \frac{\sum_{i=1}^{p-1}(u_{(i+1)} - u_i)(v_{(i+1)} - v_i))}{\sqrt{\sum_{i=1}^{p-1}(u_{(i+1)} - u_i)^2}\sqrt{\sum_{i=1}^{p-1}(v_{(i+1)} - v_i)^2}} \quad (2)$$

$$dH(S_1, S_2) = \max\{\max_{u\in S_1}\min_{v\in S_2}\|u - v\|, \max_{v\in S_2}\min_{u\in S_1}\|v - u\|\} \quad (3)$$

In each of the patients, a ROI was delineated by an expert around the lesion in the motion-corrected DCE-MRI volumes. The time-intensity curves from the voxels inside the ROI were treated as independent objects on a voxel by voxel basis.

Using $D_k$ from Eq. 1, a dissimilarity matrix was derived on a slice-wise basis for the pairwise dissimilarities of the elements from the corresponding ROI. In such a space, each element was represented by a row vector whose dimensionality was defined by the cardinality of the ROI. For an element $x$, belonging to the $n$-element ROI set $X$, the vectorial representation within the dissimilarity space is given by

$$D_k(x, X) = [D_k(x, x_1), D_k(x, x_2), \dots D_k(x, x_n)]^T \quad (4)$$

Once the dissimilarity space was constructed, the $K$-means algorithm [9] was used to group the voxels with similar perfusion patterns in the ROI into clusters. The initial centroids were calculated automatically with a preliminary clustering stage with a random $10\%$ sample. $K$-means minimizes the sum over all clusters of the within-cluster sums of point-to-cluster-centroid distances using, in this case, the squared Euclidean distance. The $K$ number of clusters was heuristically set to $5$ taking into account the expected perfusion zones of the lesion and the surrounding tissue.

### 2.3. Registration

Given a fixed and a moving image, the registration problem is the process of finding the optimal transformation $T(X)$ that brings the moving image $m(X)$ into spatial alignment with the fixed image $f(X)$ according to a reference metric $S(f, m \circ T)$.

Despite the advances in multi-modal medical image registration, the problem of registering between DCE-MRI and DWI has not been widely investigated and reported in the literature. Moreover, it becomes an increasingly difficult task in a highly compressible and elastic tissue like the breast, with its inhomogeneous anisotropic soft tissue, inherent non-rigid behavior and lack of solid landmarks to guide the registration as fixed references.

For the implemented protocol the DCE-MRI was set as the fixed volume and the DWI as the moving one. The DCE-MRI volume corresponding to the time point where the best contrast could be detected for both the lesion and the subregions was chosen, i.e. the one acquired two minutes after the contrast medium injection, following [3]. From the DWI data, the non-diffusion weighted volume, the so called $b0$, was used as the moving one since it is less subjected to gradient-related artifacts and it is also the one providing the same amount of information on all the structures under investigation.

Due to the highly different contrast and intensity characteristics of both modalities, as well as the low resolution of the DWI volumes, the registration protocol was divided into two steps, each one following a multi-resolution strategy. In the first step, rigid and affine transformations were performed successively as substeps in order to align and match the features of the fixed and moving images. In the second step, a localized multi-resolution cubic B-spline transformation with a regularization penalty was performed to elastically refine the alignment. Normalized mutual information (NMI) was used as registration metric. NMI assumes a relation between the probability distributions of the intensities of the fixed and the moving image and is well suited for multi-modal registration. A bending energy penalty, which is based on the spatial derivatives of the transformation, was used to regularize the deformation, as detailed in [10].

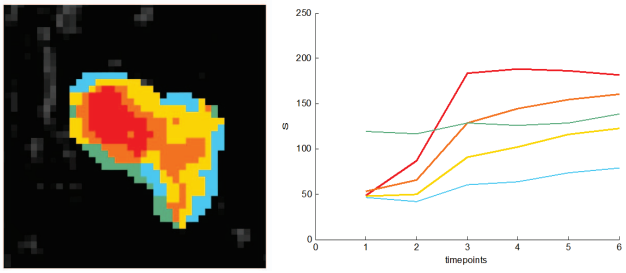



**Fig. 2**. (a) clustering of the tumoral subregions and surrounding tissue (b) average time-intensity perfusion curves within each cluster

## 3. RESULTS

The regions resulting from dissimilarity based clustering were rendered as semitransparent colored maps overlapping on the morphological images for each slice, as illustrated in Fig. 2 (a). Plots of the average time-intensity perfusion curves within each cluster highlight the inter-cluster differences (Fig. 2 (b)). The resulting clusters were analyzed by the radiologists of our team who confirmed and validated the segmentation of both the central and surrounding tumoral regions. The central region exhibits a characteristic pattern of high vascularization in the perfusion time-intensity curves, which is reflected in a high early enhancement followed by a rapid washout, indicative of angiogenesis (Fig. 2 (b), green line). Typically, surrounding this central region lays a cluster featuring a pattern of enhancement followed by a signal plateau (Fig. 2 (b), blue line). The boundary cluster surrounding these two central regions features a low enhancement behavior (Fig. 2 (b), yellow and magenta lines). Once the registration protocol was applied to the $b0$ images and validated for each subject through visual inspection, the resulting transformation was applied to the remaining $b$-values in order to calculate the transformed ADC. The clusters obtained on the DCE were projected onto the spatially registered ADC maps to perform the statistical analysis. Normality tests (Jarque-Bera) revealed that the ADC value for the different clusters analyzed was not normally distributed. Accordingly, a non parametric test (Wilcoxon-signed-rank test) was used ($p = 0.05$)

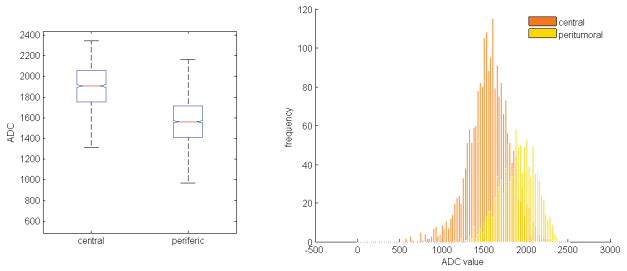



**Fig. 3**. (a) box plot showing the difference between the central and surrounding subregions (b) histograms of the 2 tumor subregions, showing the different ADC values distribution

to evaluate whether the tumors subregions clustered on the DCE corresponded to regions in the DWI whose PDFs were statistically different. In particular, separate analysis for single slices (intra-slice) and the tumor as a whole (inter-slice) were performed. In this we found that the distributions of the ADC values in the DCE-MRI defined regions were statistically different, in each one of the two conditions, in 15 out of 17 patients. Fig. 3 provides an example by showing the box plots corresponding to the tumor central and surrounding subregions (labeled as 0 and 1, respectively) of the whole volumes for one of the patients analyzed. The two lesions that showed similar ADC distributions in the different subregions were characterized by a partially flattened pattern of high vascularization in the perfusion time-intensity curves, more similar to the surrounding tissue enhancement pattern.

## 4. CONCLUSIONS

In this paper, we presented a methodology for integrating diffusion and perfusion MRI images of the breast for surgical planning. While DCE-MRI methods highlights the lesion angiogenesis, DWI allows one to non-invasively probe the ADC and thus to characterize the nature and cellularity of the lesions. A two step process for the integration of these modalities was proposed. First, dissimilarity-based clustering was performed on selected DCE-MRI images to identify the different contrast-enhancement patterns inside the tumor. The resulting regions were then mapped onto the DWI following the outcome of multi-modal registration. The PDFs of the subregions in the ADC map identified in this way were extracted and compared through non-parametric statistical testing. Our results show that subregions corresponding to different clusters in the DCE volume hold statistically different ADC characteristics, supporting the self-consistency of the method and allowing for the integration of the information obtained from the two modalities. This also suggests the exploitation of this information into the registration process through the definition of an *ad-hoc* multi-modal objective function.

## 5. REFERENCES

[1] Morrow, M., Strom, E. A., Bassett, L. W., et al., "Standard for Breast Conservation Therapy in the Management of Invasive Breast Carcinoma". CA: A Cancer Journal for Clinicians, 52: 277-300, 2002.

[2] Mameri, C. S., Kemp, C., Goldman, S. M., Sobral, L. A. and Ajzen, S., "Impact of Breast MRI on Surgical Treatment, Axillary Approach, and Systemic Therapy for Breast Cancer". Breast J, 14: 236-244, 2008.

[3] Degani, H., Gusis, V., Weinstein, D., et al., "Mapping pathophysiological features of breast tumors by MRI at high spatial resolution". Nat Med, 3(7):780-782, 1997.

[4] Gal, Y., Mehnert, A., Bradley, A., et al., "Feature and Classifier Selection for Automatic Classification of Lesions in Dynamic Contrast-Enhanced MRI of the Breast". Digital Image Computing: Techniques and Applications pp.132-139, 2009.

[5] Kuhl, C.K., Mielcareck, P., Klaschik, S., et al., "Dynamic breast MR imaging: are signal intensity time course data useful for differential diagnosis of enhancing lesions?" Radiology, 211(1):101-10, April 1999.

[6] Lavini, C., de Jonge, M.C., van De Sande, M.G.H., et al., "Pixel-by-pixel analysis of DCE MRI curve patterns and an illustration of its application to the imaging of the musculoskeletal system". Magn Resonance Imaging, 25(5):604-12, June 2007.

[7] Pekalska, E., and Duin, R.P.W., "The dissimilarity representation for pattern recognition: foundations and applications". Word Scientific, Vol.64, 2005.

[8] Pekalska, E., Paclik, P., and Duin, R.P.W., "A generalized kernel approach to dissimilarity-based classification". J Mach Learn Res, 2:211, 2002.

[9] Rui, X. and Wunsch, D., "Survey of clustering algorithms". IEEE T Neural Netw, 16:645-78, 2005.

[10] Klein, S., Staring, M., Murphy, K., at al., "elastix: a toolbox for intensity based medical image registration". IEEE T Med Imaging, vol. 29, no. 1, pp. 196-205, January 2010.

[11] Douzal-Chouakria, A., Amblard, C., "Classification trees for time series". Pattern Recognition 45(3): 1076-1091, 2012

[12] Douzal-Chouakria, A., Nagabhushan, P.,"Adaptive dissimilarity index for measuring time series proximity". St Class Dat Anal 1(1):5-21, 2007